Journal of The Electrochemical Society, **158** (5) J150-J154 (2011)
0013-4651/2011/158(5)/J150/5/$28.00 © The Electrochemical Society

The Effects of Ultraviolet Exposure on the Device Characteristics of Atomic Layer Deposited-ZnO:N Thin Film Transistors

Jae-Min Kim,[a] S. J. Lim,[b] Taewook Nam,[a] Doyoung Kim,[a] and Hyungjun Kim[a,*,z]

[a]*School of Electrical and Electronic Engineering, Yonsei University, Seoul, 120-749, Korea*
[b]*Department of Materials Science and Engineering, Pohang University of Science and Technology, Pohang 790-784, Korea*

We investigated the effects of ultraviolet (UV) light illumination on nitrogen-doped atomic layer deposited (ALD)-ZnO:N thin film transistors (TFTs). ALD ZnO:N thin films grown at 125°C were used as active layers for back-gate TFT devices. As-fabricated ALD ZnO:N TFTs showed proper drain current modulation response to a gate voltage sweep with a 5.4 V threshold voltage and a clear pinch-off. However, the threshold voltage was significantly shifted in the negative direction by UV exposure due to an associated increase in carrier concentration, resulting in the loss of current modulation by gate voltage sweep. In addition, we observed a resistivity change in ALD ZnO:N thin films with time after UV exposure. The resistivity decreased by several orders of magnitude upon UV light exposure and recovered toward its original value after switching off the UV light. Accordingly, the transfer curves of TFT devices using a ZnO:N active layer also exhibited recovery characteristics. We formed a thin Al_2O_3 passivation layer on top of the TFT surface in order to suppress the recovery effect.
© 2011 The Electrochemical Society. [DOI: 10.1149/1.3560191] All rights reserved.

Manuscript submitted November 9, 2010; revised manuscript received January 21, 2011. Published March 15, 2011. This was Paper 1790 presented at the Las Vegas, Nevada, Meeting of the Society, October 10–15, 2010.

In recent years, the demand for transparent thin film transistors (TFTs) has enormously increased for next generation transparent displays such as transparent organic light emitting diodes, heads-up displays, and smart windows.[1] To meet this demand, oxide semiconductors have been extensively studied to replace conventional Si-based TFTs mainly due to their high transparency to visible light and good electrical properties.[2–4] Particularly, polycrystalline zinc oxide (ZnO) thin films are considered as attractive candidates because they possesses evident advantages over opaque Si-based TFTs such as high saturation mobility, high on-off current ratio, wide optical band gap, and low temperature processability.

However, since ZnO-TFTs inherently contain deep level defects in the channel/dielectric interface which act as recombination centers, they could generate an unwanted photo-current and alter film properties during light transmission and device operation, resulting in severe problems.[5–7] For example, Park et al. reported that simultaneous exposure of white light on ZnO-based TFTs underwent negative shift in threshold voltage under negative-bias stress conditions.[8] Besides, Bae et al. observed the generation of photocurrent in ZnO-based TFTs in UV illuminated condition.[9,10] Additionally, Goldberger et al. reported that UV irradiation causes changes in the electrical properties of ZnO field effect transistors (FETs) due to the decrease in resistivity with increasing carrier concentration.[11] However, detail electrochemical mechanisms as a result from UV illumination on ZnO-based TFTs have rarely been discussed.

In this article, we investigated the changes in device properties of ALD-ZnO:N TFTs with respect to UV light exposure. Especially, we concentrate on the electrochemical mechanisms in occurrence with UV illumination with ZnO surface analysis to support the anticipated phenomena. We previously reported that TFT devices with an atomic layer deposited (ALD)-, nitrogen-doped ZnO thin film active layer show excellent characteristics of high μ_{sat} (6.7 $cm^2/V\ s$) and $I_{on/off}$ ($\sim 10^8$).[12] A significant negative shift in the threshold voltage (V_{TH}) was observed after UV exposure, indicating an increase in carrier concentration in the ZnO channel area. However, this change was fully recovered to its original state after switching off the UV light when the device was exposed in air without a surface passivation layer. In contrast, we adopted a thin Al_2O_3 passivation layer on the top surface of the TFT and observed that the recovery was effectively suppressed.

Experimental

ALD-ZnO:N thin films were deposited using a home-made hot wall-type ALD reactor with diethyl zinc (DEZ) (Epichem adduct grade) as a precursor and diluted ammonium hydroxide (NH_4OH) solution (0.01%) as a single source for both oxygen and nitrogen (via ammonia) doping. The growth temperature was maintained at 125°C during the ALD process using a ceramic heater located under the graphite substrate holder. The flow of Ar carrier gas with precursor molecules was controlled by a needle valve to maintain an operating pressure of 160 mTorr during the DEZ exposure step. Argon gas (99.99% purity) was used as a purging and a carrier gas, and the flow was controlled by a mass flow controller (5 sccm for DEZ bubbler and 20 sccm for purging). A typical ALD process is composed of four consecutive steps: DEZ exposure for 2 s, Ar purging for 8 s, NH_4OH exposure for 3 s, and Ar purging for 4 s. The thicknesses of the films were routinely measured using an ellipsometer (Rudolph auto ELII), and resistivity was measured using a four-point probe with a source meter (Keithley 2400).

To investigate the UV exposure effects on the device properties, we prepared inverted, staggered-type ALD-ZnO:N TFT devices (with bottom gate and top contact) on an n^+ Si substrate, also used as the gate electrode. First, 100-nm-thick ALD-Al_2O_3 was deposited as a gate insulator using trimethyl aluminum (TMA) and water vapor at a growth temperature of 150°C. Then, a 66-nm-thick ZnO:N active layer was prepared using the ALD process mentioned above. The active channel area was defined using a standard lithographic process with AZ-5214 as a PR material, followed by wet etching with a diluted HCl solution ($HCl:H_2O = 1:40$). The channel width and length of the device were confined to be 40 and 20 μm, respectively. Finally, a 100-nm-thick Ti layer was deposited and patterned via lift-off using magnetron sputtering for the source/drain contact. The schematic configurations of the tilt and top view of the TFT device are shown in Fig. 1.

After the device preparation, UV light was applied for 0, 5, and 30 min under vacuum conditions using a specially designed UV exposure system maintained at 50 mTorr base pressure via a mechanical pump. The wavelength and the illumination power of the UV light used in this study were 368 nm and 0.1 mW/m^2, respectively. The characteristics of ZnO:N TFTs, including transfer and output curves, during UV exposure were measured using a Keithley 4200 semiconductor parameter analyzer with three probes.

To investigate the resistivity changes in the ZnO:N thin films post-UV exposure in ambient air, we prepared 66-nm-thick ALD-ZnO:N films on glass (Corning 1737) substrates followed by

* Electrochemical Society Active Member.
z E-mail: hyungjun@yonsei.ac.kr

Downloaded on 2015-06-24 to IP 157.182.150.22 address. Redistribution subject to ECS terms of use (see ecsdl.org/site/terms_use) unless CC License in place (see abstract).

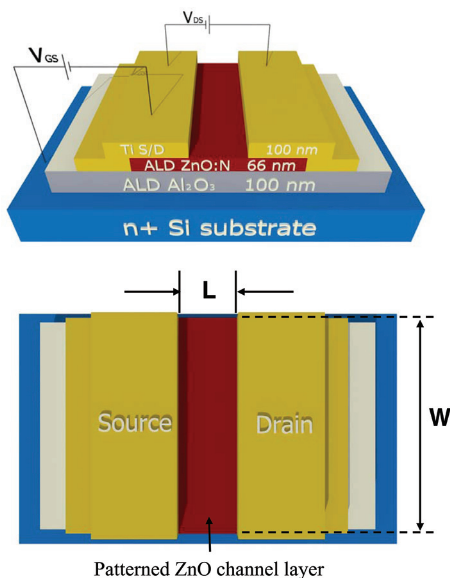

Figure 1. (Color online) The schematic drawing of an inverted staggered type TFT using ALD-ZnO:N as an active layer.

patterning of 100-nm-thick Ti electrodes using sputtering with a stainless steel hard mask. After sample preparation, we exposed the ZnO:N films to UV light for 30 min with the same wavelength and power as above under vacuum conditions. Then, we measured the resistivities of the ZnO:N thin films with increasing post-UV exposure time up to 168 h (1 week) after breaking the vacuum. Additionally, X-ray photoemission spectroscopy (XPS) was conducted to analyze the changes in the chemical bonding states of oxygen molecules on the surfaces of the ZnO:N films as a function of UV exposure time without surface cleaning via Ar sputtering.

For experiments on the recovery of ALD ZnO:N TFT characteristics, UV was applied for 30 min to the devices with and without an Al_2O_3 passivation layer, and the transfer curves were measured immediately after UV exposure and after 168 h in air. The passivation layer, i.e., a 30-nm-thick ALD-Al_2O_3 thin film, was deposited at $T_s = 150°C$ on top of the TFT surface layer.

Results and Discussion

The effects of UV exposure on ZnO:N TFT devices.—As we have previously reported, undoped ALD-ZnO thin films prepared at $T_s = 150°C$ have a low resistivity of several Ω cm due to a large n-type carrier concentration greater than 10^{17} cm^{-3}, resulting in non-operative TFT devices.[12] However, the resistivity increased to more than 1500 Ω cm after nitrogen doping due to a decrease in carrier concentration using 0.01% NH_4OH as a reactant. As a result, the device exhibited a clear pinch-off and current saturation with good device characteristics of high saturation mobility (6.7 cm^2/Vs) and on/off current ratio ($\sim 10^8$).

Here, we investigated the changes in device properties of ALD-ZnO:N TFT with respect to UV exposure. The transfer and output curves as a function of exposure time are shown in Figs. 2 and 3, respectively. The device with no UV exposure was well modulated by a gate voltage sweep and exhibits hard saturation, evidenced by the flatness of the slope of each curve, indicating that the entire thickness of the ZnO channel layer can be depleted. The threshold voltage (V_{TH}) and saturation current (I_{Sat}) were 5.4 V and 21 μA, respectively, at $V_{DS} = 30$ V for $V_G = 30$ V. Furthermore, the device operated in enhancement mode, exhibiting normally-off characteristic. However, the transfer curves after UV exposure for 5 min showed significant negative shifts in V_{TH} from 5.4 to −10.5 V. After a UV exposure of 30 min, the device could not be turned off even with a −35 V gate voltage at a 5 V source/drain voltage

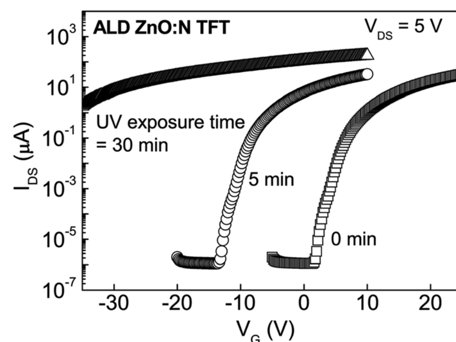

Figure 2. The changes in transfer curves for ALD-ZnO:N TFT as a function of UV exposure time.

(V_{DS}). Further, the output curves showed an almost linear increase with V_{DS}, instead of the normal saturation behavior.

Since V_{TH} is intimately related to the carrier concentration in the channel layer, the negative V_{TH} shift may be related to an increase in electron concentration in the active layer. Thus, resistivity measurements were carried out for the UV-exposed sample, indicating that the resistivity of the as-deposited ZnO:N film with an initial resistivity of 1500 Ω cm significantly decreased to 5 Ω cm after UV exposure for 30 min. According to previous reports,[10,13–16] the increase in electron concentration in ZnO as a result of UV exposure can be explained by the generation of oxygen vacancies denoted by

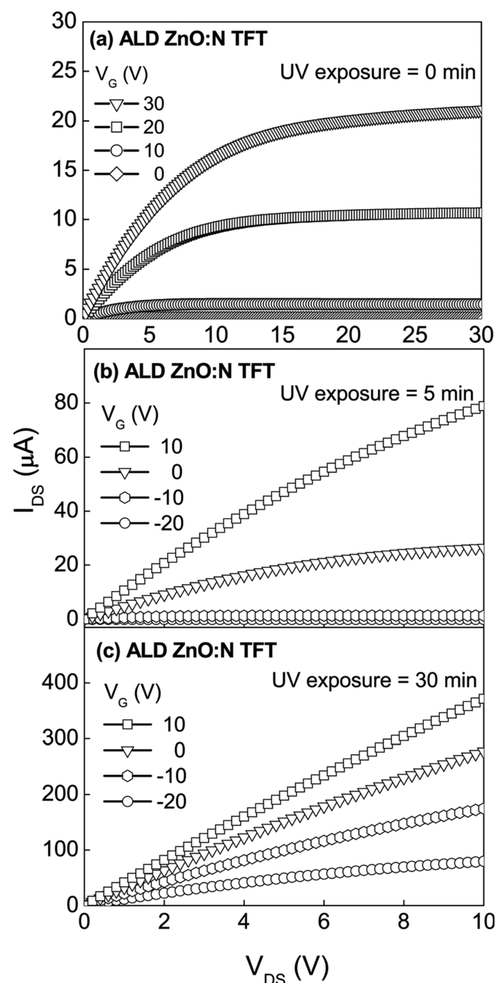

Figure 3. The changes in output curves for ALD-ZnO:N TFT as a function of UV exposure time for (a) 0 min, (b) 5 min, and (c) 30 min.

Downloaded on 2015-06-24 to IP 157.182.150.22 address. Redistribution subject to ECS terms of use (see ecsdl.org/site/terms_use) unless CC License in place (see abstract).

V_O''. Incident UV light, which possesses higher energy than the bandgap energy of ZnO, can generate electron-hole pairs due to band-to-band excitation. The generated holes are consumed by the desorption of oxygen ions in the ZnO lattice near the surface, resulting in the creation of V_O'' through the following reactions

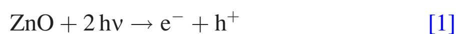

$$ZnO + 2\,h\nu \rightarrow e^- + h^+ \quad [1]$$

$$O^{2-} + h^+ \rightarrow O^- \quad [2]$$

$$O^- + h^+ \rightarrow 1/2O_2(g) + V_O'' + 2e^- \quad [3]$$

Consequently, desorption of an oxygen ion creates free carriers in the form of $2e^-$, which results in significant V_{TH} decreases in ZnO TFTs. Also, it is well known that the holes in ZnO-based semiconductors exhibit strong localization at oxygen 2p levels or in an upper edge of the valence band due to the highly electronegative nature of oxygen.[17–20] Thus, it is worth mentioning that photo-generated holes under UV illumination tend to be localized to regions rich in oxygen, exhibiting more electron trapping in the channel layer. Consequently, a more negative gate voltage is required to deplete electron carriers from the channel layer in order to turn off the TFT device.[14] This explanation is in agreement with our TFT characteristic measurement results. Thus, ZnO:N TFTs after UV exposure for 30 min cannot operate properly due to the generation of excess electrons.

Post-exposure recovery effects.—Next, the effects of air exposure on the electrical properties of ALD-ZnO:N thin films after turning off the UV light were investigated. Figs. 4 shows the resistivity change in the 30 min UV-exposed ALD-ZnO:N film with post-UV exposure time in air. For the initial 30 h, the resistivity remained at a relatively constant value of 5 Ω cm and then increased gradually, reaching 600 Ω cm after 168 h (1 week), illustrating recovery toward its original value before UV exposure. This recovery behavior of the film resistivity can be explained by the surface adsorption of oxygen molecules from an oxygen source, such as water vapor in ambient air, which reduces the oxygen vacancies in ZnO films and decreases carrier concentration. As previously mentioned, holes generated by UV exposure under vacuum condition are consumed by desorption of oxygen ions, resulting in the creation of V_O'' in the ZnO surface. However, when the UV-treated samples are exposed to air, the generated V_O'' act as adsorption sites for oxygen sources, leading to the following adsorption reaction[21]

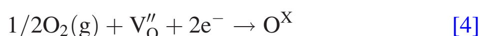

$$1/2O_2(g) + V_O'' + 2e^- \rightarrow O^X \quad [4]$$

As a result, the adsorption of the oxygen to the V_O'' defect sites destroys the free carrier $2e^-$, resulting in an increase in the resistivity of ZnO film, as shown in Fig. 4.

The defective site, V_O'', is known to be a favorable adsorption site for water molecules (H_2O) and hydroxyl groups (OH^-).[11,22] Sun *et al*. observed that dissociatively adsorbed water molecules (OH^-) are preferable adsorbents to physically adsorbed water molecules (H_2O).[10] Also, Feng et al. showed the effect of the increase in OH^- concentration on the defect sites under UV illumination when surrounded by water molecules.[23] Likewise, we observed the existence of hydroxyl groups on the surfaces of ALD-ZnO:N films using XPS. Fig. 5a shows the XPS spectra of the O 1s binding energy region for ZnO:N films after exposure by UV light for 0, 5, and 30 min. It should be noted that the XPS measurements were conducted 50 h after the samples were removed from the UV exposure chamber. All of the three XPS spectra contain two peaks at 530.5 and 532.3 eV, corresponding to O-Zn and O-H bonding, respectively. Even in the unexposed sample, a peak for O-H bonding is observed. This is a general observation for ZnO films deposited using various techniques including sputtering, pulsed laser deposition (PLD), spray pyrolysis, and chemical vapor deposition (CVD).[10,24–27] However, we observed that the relative intensity between O-H and O-Zn bonding (O-H/O-Zn) was increased for the film exposed to UV light for a longer time, as shown in Fig. 5b. The longer the sample was exposed to UV light, the larger was the number of photo-generated oxygen vacancies created by the desorption mechanism, which, as mentioned previously, provides a higher density of adsorption sites for water molecules on ZnO surfaces.

Since the UV exposure was conducted under vacuum, there is little possibility that the adsorption of existing water molecules occurs at oxygen vacancy sites during the exposure step. Meanwhile, if the sample was exposed to water in air ambient after extracting the sample from the UV chamber, it would cause a chemisorption process of oxygen vacancies with water molecules, leading to the formation of hydroxyl bonding on the ZnO surface. Hence, it is reasonable to consider that the increased adsorption sites on a UV-illuminated ZnO surface enhance the reaction rate for the recovery of oxygen vacancies through an adsorption mechanism, resulting in an additional increase in the O-H level compared to those of samples not exposed to UV. This result provides a strong basis for the recovery behavior observed in ZnO:N films.

The recovery of electrical properties in ZnO:N thin films due to air exposure produces significant effects on TFT device properties. Figure 6 shows the shift in transfer curves of ZnO:N TFT with

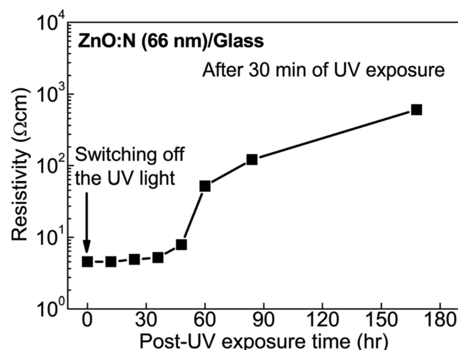

Figure 4. The resistivity change in 30 min UV-exposed ALD-ZnO:N thin film with increasing post-UV exposure time.

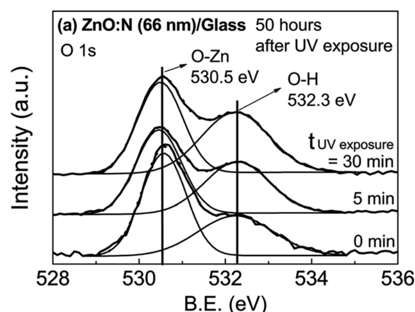

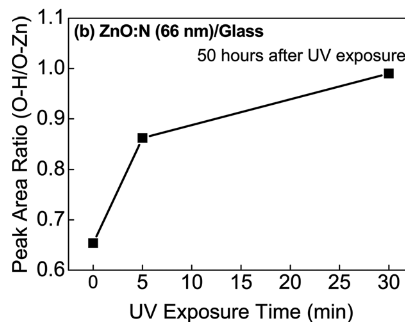

Figure 5. (a) The XPS spectra of the O 1s peak of ALD-ZnO:N thin films 50 h after UV exposure for 0, 5, and 30 min. (b) The peak area ratio (O-H/O-Zn) of each sample.

Downloaded on 2015-06-24 to IP 157.182.150.22 address. Redistribution subject to ECS terms of use (see ecsdl.org/site/terms_use) unless CC License in place (see abstract).

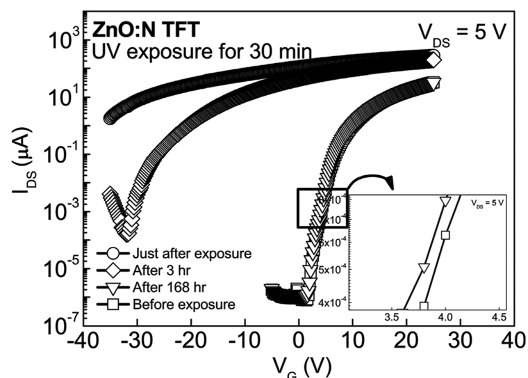

Figure 6. The time dependence of transfer curve change for ALD-ZnO:N TFT after 30 min of UV exposure.

respect to post-UV exposure times of 0, 3, 168 h in ambient air. As mentioned previously, UV exposure for 30 min causes a significant negative V_{TH} shift, resulting in improper operation of the device. However, we observed that this negatively shifted transfer curve slowly recovers to its original state (before UV exposure) with time after deactivating the UV light. Three hours after exposure, the device began to be modulated properly by a gate voltage sweep with $V_{TH} = -21.1$ V. Moreover, the transfer curve returned to its initial state 168 h after exposure. It should be noted that the V_{TH} obtained at 168 h after UV exposure has the same value with that before UV exposure as to 5.4 V.

For comparison, we prepared ZnO:N TFT devices passivated with 30-nm-thick ALD-Al_2O_3, and we subsequently exposed them to UV for the same time and conditions as those in the control sample. Then, we measured the changes in the transfer curves of the device with respect to post-UV exposure time in order to investigate the effects of the passivation layer on the recovery characteristics. The specific purpose of the Al_2O_3 passivation layer is to block the ZnO channel layer from air exposure. Experimental results are summarized in Fig. 7. The device operated well with a gate bias according to the transfer curve for the TFT before UV exposure with $V_{TH} = 5.0$ V. However, modulation by the gate bias was not observed within the sweeping range after UV exposure for 30 min due to a large negative V_{TH} shift, the same behavior as was seen with the unpassivated ZnO:N TFTs.

However, in the post-UV exposure recovery regime, the result was different from that of the controlled sample. Specifically, the device with a passivation layer still did not exhibit source-drain current modulation by a gate bias sweep even 3 h after exposure. We only observed that the device showed the proper TFT transfer characteristic 168 h after UV exposure with -2.0 V of V_{TH} but still did not fully recover to its original state. This result confirms that an Al_2O_3 passivation layer effectively retarded the recovery of

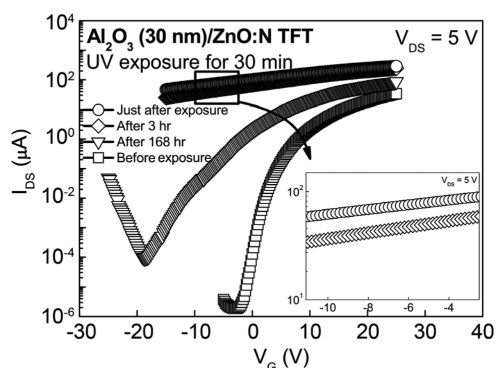

Figure 7. The time dependence of transfer curve change for ALD ZnO:N TFT with a 30-nm-thick ALD-Al_2O_3 passivation layer after 30 min of UV exposure.

Table I. The time dependence of device property change for ALD-ZnO:N TFT (a) without and (b) with an Al_2O_3 passivation layer after 30 min of UV exposure.

The time after UV exposure	Before UV exposure	Just after UV exposure	After 3 h	After 168 h
(a) UV exposure for 30 min on ZnO:N TFT without passivation layer				
V_{TH} (V)	5.4	—	–21.1	5.4
S (V/dec)	0.5	—	0.9	0.5
μ_{sat} (cm^2/Vs)	1.4	1.1	1.2	1.4
I_{OFF} (pA)	1.12	—	161	1.06
$I_{ON/OFF}$	1.9×10^7	—	1.0×10^6	7.3×10^6
(b) UV exposure for 30 min on ZnO:N TFT with passivation layer				
V_{TH} (V)	5	—	—	−2
S (V/dec)	0.95	—	—	0.5
μ_{sat} (cm^2/Vs)	1.2	1.5	1.4	1.6
I_{OFF} (pA)	1.7	—	—	98
$I_{ON/OFF}$	1.8×10^7	—	—	9.3×10^5

UV-exposed TFT characteristics. Generally, ZnO exhibits strong chemisorption with molecules in the surrounding environment, especially oxygen-containing gaseous species, resulting in a change in conductivity.[28,29] Thus, this slow recovery behavior can be explained by the thin passivation layer prohibiting the chemisorption of water molecules and hydroxyl groups as a source for oxygen to recover oxygen vacancies in ZnO lattice. Similarly, Chang et al. reported that SiO_2/Si_3N_4 bilayer passivation on ZnO nanowires showed superior FET performance relative to that of unpassivated ZnO, which was attributed to the reduction in surface chemisorptions processes at oxygen vacancy sites.[30]

Tables I(a) and I(b) summarize the device parameter changes according to the recovery behavior of ZnO:N TFT as described in Figs. 6 and 7, respectively. While the saturation mobility remained almost constant at around $\sim$1.3 cm^2/V s, regardless of post-UV exposure time, the photo-induced off-current was greatly increased in both cases. For example, the I_{OFF} for the TFT without passivation layer 3 h after UV exposure was 161 pA, 2 orders of magnitude higher than that before UV exposure. It is well known that UV light generates photo-induced carriers in ZnO, providing higher current than that in the normal state.[31–34] Thus, this result can be explained by the withdrawal of electrons generated through UV illumination to the back channel area of the ZnO film, contributing to the increase in off-current.

Conclusion

In conclusion, we investigated the changes in ALD-ZnO:N TFT characteristics with respect to UV exposure time and post-exposure time. We have shown that the V_{TH} of the device shifts in the negative direction with increasing UV exposure. Although the resistivity of ZnO:N thin film after UV exposure for 30 min had a much lower value than that before UV exposure, it tended to increase toward its initial value. The XPS spectra showed an increase in the number of hydroxyl groups on the ZnO:N film surface with increasing UV exposure time, illustrating the recovery mechanism occurring in ZnO:N films, which explains the resistivity increase with time after UV exposure. Also, we compared the recovery behaviors of ZnO:N TFTs with and without an Al_2O_3 passivation layer. Although the transfer curve of the device completely recovered to its original state with increasing post-exposure time, the use of a thin passivation layer effectively suppressed this phenomenon.

Acknowledgments

This research was supported by the Future-based Technology Development Program (Nano Fields) and Basic Research Program through the National Research Foundation of Korea (NRF) funded by the Ministry of Education, Science and Technology (No. 2010-

Downloaded on 2015-06-24 to IP 157.182.150.22 address. Redistribution subject to ECS terms of use (see ecsdl.org/site/terms_use) unless CC License in place (see abstract).

0020230 and 2010-0024066). Also, this work was supported by the Yonsei University Research Fund of 2010 (No. 2009-1-0195 and 2009-1-0233).

Yonsei University assisted in meeting the publication costs of this article.

References

1. J. F. Wager, *Science*, **300**, 1245 (2003).
2. K. Nomura, H. Ohta, A. Takagi, T. Kamiya, M. Hirano, and H. Hosono, *Nature*, **432**, 488 (2004).
3. K. P. Sang-Hee, H. Chi-Sun, R. Minki, Y. Shinhyuk, B. Chunwon, S. Jaeheon, L. Jeong-Ik, L. Kimoon, O. Min Suk, and I. Seongil, *Adv. Mater.*, **21**, 678 (2009).
4. S. J. Lim, K. Soon-ju, K. Hyungjun, and P. Jin-Seong, *Appl. Phys. Lett.*, **91**, 183517 (2007).
5. H. S. Bae and S. Im, *J. Vac. Sci. Technol. B*, **22**, 1191 (2004).
6. R. J. Collins and D. G. Thomas, *Phys. Rev.*, **112**, 388 (1958).
7. R.-D. Sun, A. Nakajima, A. Fujishima, T. Watanabe, and K. Hashimoto, J. Phys. Chem. B, **105**, 1984 (2001).
8. J. S. Park, T. S. Kim, K. S. Son, J. S. Jung, K.-H Lee, J.-Y. Kwon, B. Koo, and S. Lee, *IEEE Electron Device Lett*. **31**, 440 (2010).
9. H. S. Bae and S. Im, *Thin Solid Films*, **469**, 75 (2004).
10. H. S. Bae, C. M. Choi, J. Hoon Kim, and S. Im, *J. Appl. Phys*. **97**, 076104 (2005).
11. J. Goldberger, D. J. Sirbuly, M. Law, and P. Yang, *J. Phys. Chem. B*, **109**, 9 (2004).
12. S. J. Lim, J.-M. Kim, D. Kim, S. Kwon, J.-S. Park, and H. Kim, *J. Electrochem. Soc.*, **157**, H214 (2010).
13. D. H. Zhang and D. E. Brodie, *Thin Solid Films*, **238**, 95 (1994).
14. K. Takechi, M. Nakata, T. Eguchi, H. Yamaguchi, and S. Kaneko, *Jpn. J. Appl. Phys.*, **48**, 010203 (2009).
15. R. L. Hoffman, B. J. Norris, and J. F. Wager, *Appl. Phys. Lett.*, **82**, 733 (2003).
16. H. Y. Hannes Kind, B. Messer, M. Law, and P. Yang, *Adv. Mater.*, **14**, 158 (2002).
17. J.-L. Zhao, X.-M. Li, A. Krtschil, A. Krost, W.-D. Yu, Y.-W. Zhang, Y.-F. Gu, and X.-D. Gao, *Appl. Phys. Lett.*, **90**, 062118 (2007).
18. H. Yanagi, S.-i. Inoue, K. Ueda, H. Kawazoe, H. Hosono, and N. Hamada, *J. Appl. Phys.*, **88**, 4159 (2000).
19. A. N. Banerjee and K. K. Chattopadhyay, *Prog. Cryst. Growth Charact. Mater.*, **50**, 52 (2005).
20. U. Ozgur, Y. I. Alivov, C. Liu, A. Teke, M. A. Reshchikov, S. Dogan, V. Avrutin, S. J. Cho, and H. Morkoc, *J. Appl. Phys.*, **98**, 041301 (2005).
21. S. E. Ahn, J. S. Lee, H. Kim, S. Kim, B. H. Kang, K. H. Kim, and G. T. Kim, *Appl. Phys. Lett.*, **84**, 5022 (2004).
22. R. Wang, N. Sakai, A. Fujishima, T. Watanabe, and K. Hashimoto, *J. Phys. Chem. B*, **103**, 2188 (1999).
23. X. Feng, L. Feng, M. Jin, J. Zhai, L. Jiang, and D. Zhu, *J. Am. Chem. Soc.*, **126**, 62 (2003).
24. H. Xu, Y. Liu, C. Xu, Y. Liu, C. Shao, and R. Mu, *Appl. Phys. Lett.*, **88**, 242502 (2006).
25. T. P. Smith, W. J. Mecouch, P. Q. Miraglia, A. M. Roskowski, P. J. Hartlieb, and R. F. Davis, *J. Cryst. Growth*, **257**, 255 (2003).
26. L. Mar, P. Timbrell, and R. Lamb, *Thin Solid Films*, **223**, 341 (1993).
27. S. Park, T. Ikegami, and K. Ebihara, *Thin Solid Films*, **513**, 90 (2006).
28. M. Liu and H. K. Kim, *Appl. Phys. Lett.*, **84**, 173 (2004).
29. J. Lagowski, J. E. S. Sproles, and H. C. Gatos, *J. Appl. Phys.*, **48**, 3566 (1977).
30. P.-C. Chang, Z. Fan, C.-J. Chien, D. Stichtenoth, C. Ronning, and J. G. Lu, *Appl. Phys. Lett.*, **89**, 133113 (2006).
31. H. S. Bae, M. H. Yoon, J. H. Kim, and S. Im, *Appl. Phys. Lett.*, **83**, 5313 (2003).
32. A. Solbrand, A. Henningsson, S. Sodergren, H. Lindstrom, A. Hagfeldt, and S.-E. Lindquist, *J. Phys. Chem. B*, **103**, 1078 (1999).
33. Y. Ushio, M. Miyayama, and H. Yanagida, *Jpn. J. Appl. Phys.*, **33**, 1136 (1994).
34. V. Subramanian, E. E. Wolf, and P. V. Kamat, *J. Phys. Chem. B*, **107**, 7479 (2003).

Downloaded on 2015-06-24 to IP 157.182.150.22 address. Redistribution subject to ECS terms of use (see ecsdl.org/site/terms_use) unless CC License in place (see abstract).